Article:
Tang, Xinke, Chen, Zhen, Zhao, Zongyao et al. (2 more authors) (2022) Experimental study on underwater continuous-variable quantum key distribution with discrete modulation. Optics Express. pp. 32428-32437. ISSN: 1094-4087

https://doi.org/10.1364/OE.464659

Research Article | Vol. 30, No. 18 / 29 Aug 2022 / Optics Express 32428
Optics EXPRESS

Experimental study on underwater continuous-variable quantum key distribution with discrete modulation

XINKE TANG,[1] ZHEN CHEN,[1] ZONGYAO ZHAO,[1,2] RUPESH KUMAR,[3,4] AND YUHAN DONG[1,2,5]

[1]*Peng Cheng Laboratory, Shenzhen 518055, China*
[2]*Shenzhen International Graduate School, Tsinghua University, Shenzhen 518055, China*
[3]*Quantum Communications Hub and York Centre for Quantum Technologies, School of Physics, Engineering and Technology, University of York, YO10 5DD, UK*
[4]*rupesh.kumar@york.ac.uk*
[5]*dongyuhan@sz.tsinghua.edu.cn*

Abstract: We experimentally demonstrated the feasibility of an underwater continuous-variable quantum key distribution (CV-QKD) system based on four-state protocol, which is promising to guarantee the unconditionally secure underwater wireless optical communication. CV-QKD parameter estimation is performed after transmitting quantum coherent signal from Alice to Bob through a water tank. The secure key rate under collective attack of the demonstrated CV-QKD system is estimated as 22.9 kbits/s at a channel loss of 12.4 dB. In addition, the performance is also investigated with various water types and the maximum underwater transmission distance of the demonstrated CV-QKD system is estimated as 148.7 m in the pure sea water.

1. Introduction

In recent years, the exploration of the ocean has gained a growing interest and the demands for human underwater activities have significantly increased [1,2]. Underwater wireless communication (UWC) technology, which enables reliable data transmission between underwater vehicles and sensors, hence plays a significant role in the realization of ocean exploration systems [1,3]. Underwater wireless optical communication (UWOC), as an effective approach to achieving high-speed data transmission within short ranges, has been recently shown as a promising complement to long-range acoustic communication and gained considerable research interest [4]. UWOC has been also normally regarded as a securer communication method over acoustic and RF communication [1,4]. Although the UWOC systems have been widely demonstrated and investigated in order to further improve the transmission distance and data rate [5], their security issue was barely studied but has been recently pointed out and demonstrated [4].

Fortunately, quantum key distribution (QKD), which is able to guarantee unconditionally secure communication, can be a promising solution to the security issues of UWOC. Since the first protocol was introduced in 1984 [6], various QKD protocols have been investigated and demonstrated over standard single-mode fiber optics as well as free-space channels [7–12]. The QKD protocols can be mainly classified into discrete variable (DV)-QKD and continuous variable (CV)-QKD [10]. In DV-QKD protocols, secure key information is encoded in the discrete values of polarization or phase of single photons. Single photon counting techniques have been employed to decode the information. The security of DV-QKD is based on the usage of the superposition of states in mutually unbiased bases that guarantees no-cloning of the states by an eavesdropper. In the case of eavesdropping, it results in the quantum bit error rate (QBER)-a threshold of which stops the secure key generation. In CV-QKD protocols, on the other hand, secure keys are encoded on the quadrature values of the electromagnetic field and decoded using

#464659 https://doi.org/10.1364/OE.464659
Journal © 2022 Received 22 May 2022; revised 25 Jul 2022; accepted 3 Aug 2022; published 19 Aug 2022

Optics EXPRESS

quantum sensitive coherent detection [13]. The security comes from the uncertainty in the quadratures measurement related to the vacuum noise (shot noise). This uncertainty- referred as Heisenberg uncertainty, prevents perfect cloning of the states by the eavesdropper. Once the vacuum noise has been calibrated by Bob, it is possible to estimate excess noise induced by the eavesdropper. Like QBER in the DV-QKD, a threshold value of excess noise in CVQKD stops secure key generation.

CV-QKD is a relatively younger technique and has been proposed about two decades later than DV-QKD. It has attracted more attention in recent years, thanks to its tolerance to the background noise, low cost and compatibility with classical optical communication components and systems [13,14]. The feasibility of underwater QKD has been studied both theoretically [15,16] and experimentally [17–21]. However, the protocols of the reported works and studies were mainly based on DV-QKD, such as BB84. Recently, underwater CV-QKD has gained more research interest due to its distinct advantages, and has been theoretically investigated and analyzed [14,22–25].

In this paper, to the best of our knowledge, we have experimentally demonstrated the feasibility of underwater CV-QKD based on four-state modulation for the first time. Effective phase correction method has been employed and tested. Shot noise performance of the balanced homodyne detector has been demonstrated and the secure key rate has been analyzed based on the experimentally estimated excess noise and transmittance via the underwater channel. The rest of the paper is organized as follows. In Section 2, the four-state protocol is introduced along with its security key rate analysis. Section 3 describes the detailed experimental setup of the underwater CV-QKD system based on the four-state modulation. The obtained experimental results are also analyzed and discussed in this section. A brief conclusion of this paper is drawn in Section 4.

2. Protocol and the secure key rate analysis

The four-state discretely modulated CV-QKD protocol that we employed in this work is proven secure against collective attacks [10,26]. The schematic diagram of the four-state CV-QKD protocol is shown in Fig. 1.

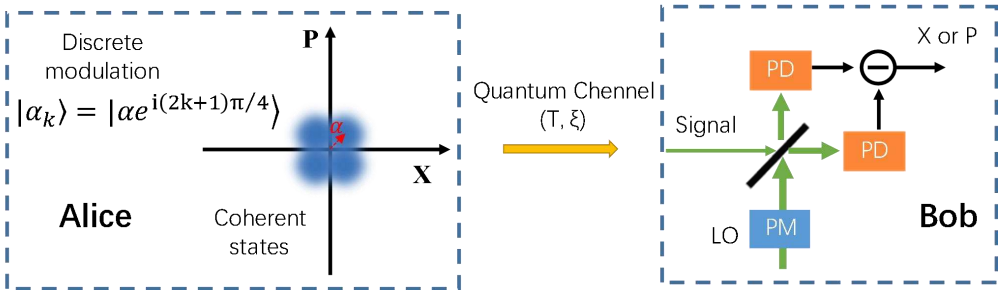

Fig. 1. Schematic diagram of the four-state CV-QKD protocol. (PD: Photodiodes ; PM: Phase Modulation)

In this protocol, the sender- Alice randomly select a number k from the set of {0,1,2,3} with equal probability and prepares the corresponding coherent state $|\alpha_k\rangle = \left|\alpha e^{i(2k+1)\pi/4}\right\rangle$. Here, α is the amplitude common to the four states and is related to the signal modulation variance V_A at Alice as $\alpha = \sqrt{(V_A/2)}$ [22,26]. Then, Alice sends the state to the receiver- Bob via a quantum channel, which can be characterized by its overall transmittance T and excess noise ξ(ie. the noise variance in excess of the shot noise). The transmittance is related to the channel attenuation and the excess noise can be due to the action of an eavesdropper. At Bob, one of the two quadrature values is randomly chosen to be measured by a balanced homodyne detection.

Optics EXPRESS

The choice of quadrature measurement is publicly announced to Alice. As a result, a sequence of correlated quadrature values is obtained and stored at both Alice and Bob. A portion of this data is revealed to estimate the channel parameters T and ξ, which are then used for evaluating the mutual information, I_{AB}, between Alice and Bob as well as the maximum amount of information, S_{BE} accessible to Eve. The final secure key information shared between Alice and Bob under collective attack can be expressed as $K = \beta I_{AB} - S_{BE}$ [10], where β is the reconciliation efficiency. The mutual information between Alice and Bob is given by [22,26,27]:

$$I_{AB} = \frac{1}{2}\log_2 \frac{V + \chi_{\text{tot}}}{1 + \chi_{\text{tot}}} \tag{1}$$

where V is defined as $V = V_A + 1$. $\chi_{tot} = \chi_{line} + \chi_{hom}/T$ is the overall noise referred to Alice, which is contributed from both the noise added in the channel $\chi_{line} = 1/T - 1 + \xi$ and the detection-added noise $\chi_{hom} = (1-\eta_B + V_{ele})/\eta_B$. η_B and V_{ele} are the transmission efficiency and electronic noise of Bob's detector, respectively. All the parameters here are implicitly expressed in the shot noise unit (SNU).

The term of S_{BE} is the maximum mutual information that Eve can access from Bob, which is limited to the Holevo bound [28].

$$S_{BE} = \sum_{i=1}^{2} G\left(\frac{\upsilon_i - 1}{2}\right) - \sum_{i=3}^{5} G\left(\frac{\upsilon_i - 1}{2}\right) \tag{2}$$

where $G(x) = (x+1)\log_2(x+1) - x\log_2 x$, the symplectic eigenvalues υ_i (i=1,2,3,4,5) are given in Appendix A [22,26].

The attenuation caused by water absorption and scattering affects the channel parameters which in turn affects the secure key generation rate. In the following sections, we experimentally study the performance of a four-state discretely modulated CV-QKD over the water channel. Specifically, by estimating the parameters T and ξ in SNU through the water channel after revealing a fraction of quadrature values hold by Alice and Bob, the secure key information of the underwater four-state modulation CV-QKD system can be evaluated based on the above equations.

3. Underwater CV-QKD with four-state modulation

In this section, we conduct the experimental study of underwater CV-QKD based on four-state modulation which shows the evidence that the four-state protocol can generate secure keys over an underwater link.

3.1. Experimental setup

Figure 2 shows the experimental setup with a water tank filled with tap water to simulate the water channel between Alice and Bob. The underwater CV-QKD can be conducted by the use of 450 nm-550 nm laser source, thanks to the existing blue-green light transmission "window" of water [1,29]. In this work, a continuous wave (CW) laser source at a wavelength of 532 nm is used as the signal source at Alice. The laser is externally modulated by an amplitude modulator and a phase modulator, randomly, in order to select one of the four coherent states in the protocol. The RF signals for the modulations are provided by an arbitrary waveform generator (AWG, AWG5202, Tektronix) and then are amplified prior to driving the modulators. The pulse width and the repetition rate of the optical signal pulses are set to 1 ns and 250 MHz, respectively. A beam splitter is used at the output of the phase modulator to simultaneously monitor the signal power as well as send the light to the water channel via the attenuator. Due to the limited length of the tank (1 meter), a highly reflective mirror with the reflectance of about 93% is installed at each end of the water tank in order to extend the transmission distance of the light through water.

Optics EXPRESS

The turbidity of water causing the channel attenuation is increased by adding Maalox ($AL(OH)_3$ and $Mg(OH)_2$) solution, which has been widely used in UWOC experiments [1,30].

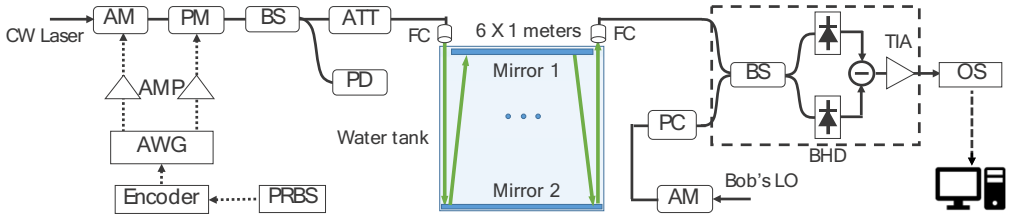

Fig. 2. Schematic of the experimental setup for feasibility study of underwater four-state modulation CV-QKD. AM: amplitude modulator; PM: phase modulator; PRBS: pseudo random bit sequence; AMP: RF amplifier; BS: beam splitter; PD: photodiode; ATT: optical attenuator; FC: fiber collimator; PC: polarization controller; OS: oscilloscope; PE: parameter estimation.

At Bob, the signals from Alice are received via a collimator. The quadrature values of the coherent states are detected by a 1 GHz balanced homodyne detector (BHD) together with a reference local oscillator (LO). In this proof-of-concept experiment, LO is generated from the same laser source. It is possible to either send the LO with the signal over the channel or generate LO locally at Bob from a second laser [31]. Another amplitude modulator is used to generate LO pulses with a fixed phase and amplitude, and also match the arrival time of the signal pulses at BHD. The intensity of LO pulses is set much higher than the signal pulses primarily to make the homodyne detection shot noise limited. High LO power also reduces the influence of background photons on homodyne detection. The polarization of the LO and signal pulses input to the BHD are mode-matched by a polarization controller. A software controlled oscilloscope (Keysight DSOS254A) is employed to capture the detected signal from BHD. The parameter estimation and the secure key rate estimation are performed offline by codes written in MATLAB.

3.2. Analysis of experimental results and secure key generation rate

After the quantum signal transmission over the water channel, Alice shares a part of her quadrature data with which Bob correlates his homodyne detection outcome. Bob also has the shot noise measurement and electronic noise calibration done before or during the quantum signal transmission. Therefore, the performance of four-state modulation CV-QKD is investigated based on the parameter estimation through the underwater channel.

The parameter estimation is performed based on the following equations [32]:

$$\mathrm{Var}(X_A) = \mathrm{Var}(P_A) = V_A \tag{3}$$

$$\langle X_A X_B \rangle = \langle P_A P_B \rangle = \sqrt{\eta_B T V_A} \tag{4}$$

$$\mathrm{Var}(X_B) = \mathrm{Var}(P_B) = \eta_B T V_A + N_0 + \eta_B T \xi + N_{\mathrm{ele}} \tag{5}$$

$$\mathrm{Var}(X_{B0}) = \mathrm{Var}(P_{B0}) = N_0 + N_{\mathrm{ele}} \tag{6}$$

where X_A and X_B are the revealed quadrature values at Alice and Bob respectively. N_{ele} is the electronic noise of the BHD. N_0 is the shot noise variance (vacuum noise fluctuation) and used as the basic unit in above equations. N_0 is experimentally measured as a function of LO power by blocking the signal port at Bob's homodyne detector but only presenting the LO to the detector. The output variance of the homodyne detector is measured at different LO power. The electronic noise variance N_{ele} is the homodyne detector output variance while LO power is zero. The outcome for shot noise measurements is shown in Fig. 3.

Optics EXPRESS

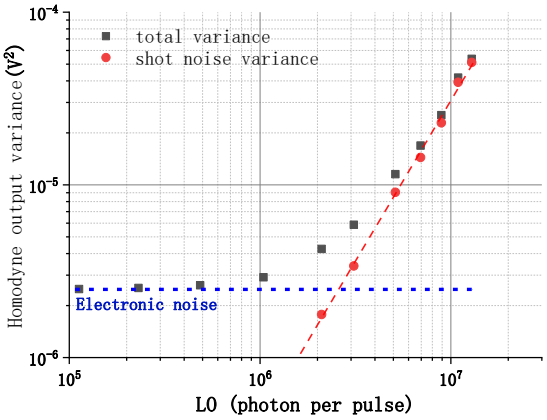

Fig. 3. Homodyne output variance as a function of LO power with zero signal. (The measured total noise and shot noise variances are shown as black dots and red dots respectively)

The total variance of output voltage from the balanced detector is contributed from both the electronic noise and shot noise as illustrated in Eq. (6). The electronic noise variance is tested as 2.48×10^{-6} V^2, which is shown as the blue dotted line. It can be seen that the total variance is nearly equal to the electronic noise when the LO power is lower than about 5×10^5 photons per pulse. As the LO power increases, the total output variance is gradually dominated by the shot noise variance and the detection becomes shot noise limited. The fitting of the shot noise variance measurements is shown as the red dotted line, which is linearly correlated with the LO power as expected. The ratio between shot noise and electronic noise are 13.14 dB, 11.99 dB and 9.64 dB at LO with 1.29×10^7, 1.09×10^7, and 8.92×10^6 photons per pulse, respectively.

Before sending the coherent states through the water channel, the value of signal variance V_A given in Eq. (3) has to be calibrated and optimized in order to obtain the maximum secure key rate. This is conducted by directly connecting Alice to Bob without the water channel. In our experiment, V_A is set to be around 0.35 SNU by the use of the optical attenuator. When the states arrive at Bob, the phase is drifted and rotated by an arbitrary angle of θ_d with respect to the phase of the LO pulses. Therefore, the CV-QKD signals are sent in packets with intense pilot pulses as packet headers. The pilot pulses carry pre-defined phase patterns which enable Bob to estimate and compensate the relative phase drift between the signal and LO. The phase estimation method is similar to that used in our recently reported work on coherent UWOC study [33]. Specifically, each packet from Alice contains 60 pilot pulses within 2^{14} total laser pulses. The pilot pulses are divided into three groups, each group with 0°, 120°, and 240°of relative phase with respect to LO, at Alice. Any phase rotation of θ_d between 0 to 360 degrees experienced by the pilot pulses can be estimated at Bob to correct the phase of the signal pulses under the assumption that pilot and signal pulses experience the same phase drift within the same packet. Figure 4 shows the phase space representation of the pilots pulses. The arbitrary phase drift of θ_d at Bob can be estimated by calculating the average quadrature values of each set of the pilot pulses based on Eq. (5) in [33]. Then, the value of θ_d is announced back to Alice for each packet. Alice makes necessary rotation on her quadrature data set to match with the quadrature detected at Bob. This compensates for the phase drift and data correlation between Alice and Bob is established.

In addition, the shot noise variance may fluctuate during the experiment, therefore it has to be measured periodically [32]. We use half of each data packet for the shot noise measurement by setting the signal transmission though amplitude modulator to null at Alice. The shot noise

Optics EXPRESS

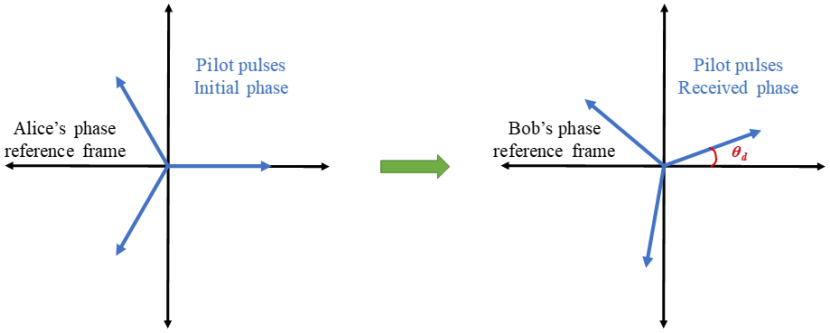

Fig. 4. Illustration of phase drift in pilot pulses. The blue arrows show the phase of the pilot pulses, which will be rotated by an arbitrary angle θ_d when the pilot pulses transmitted from Alice to Bob.

is determined as about 4.19×10^{-5} V^2 during the experiment, and the electronic noise is about 0.0593 SNU.

Next, the parameter estimation for four-state CV-QKD through the underwater channel is conducted. For simplicity, only one of the two quadrature values of coherent states is always measured, which would not affect the process and accuracy of the estimated parameters. Based on the measured quadrature values and the use of Eq. (4) and Eq. (5), the transmittance and the excess noise of the underwater CV-QKD system is obtained for the transmitted signal pulses, as shown in Fig. 5. Each of the points on the plots is an evaluation on the block size of 1.14×10^5. The overall T and ξ from the total 4.57×10^6 data points can be determined as 0.0568 and 0.0088 SNU respectively.

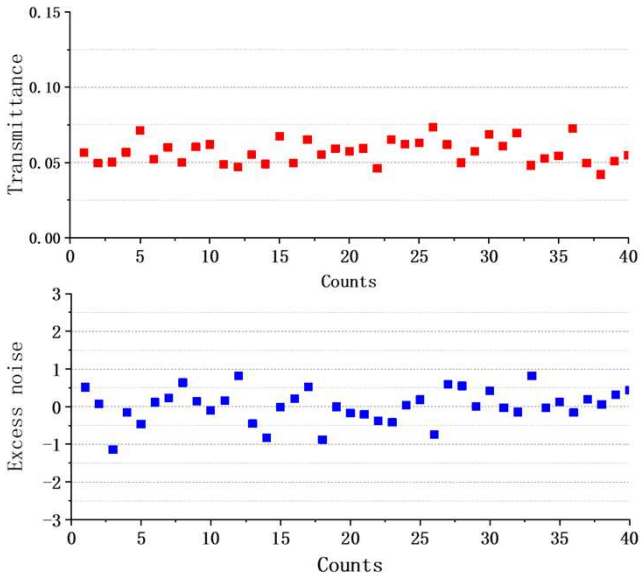

Fig. 5. Estimation of T and ξ in shot noise units for the underwater CV-QKD system.

In our experiments, the total attenuation of the 6 m water channel is measured about as 12.4 dB, and the corresponding attenuation coefficient is about 0.46/m. The overall efficiency of Bob's detector, i.e., η_B, is measured around 0.11. Based on the parameter estimation and the secure

Optics EXPRESS

key rate analysis introduced in Section 2, the corresponding secure key rate of the demonstrated system can be estimated as about 2.75 $\times 10^{-4}$ bits per pulse (corresponding to 22.9 kbits/s at the system repetition rate of 250 MHz), assuming the reconciliation efficiency of 90% and two thirds of the raw key are used for parameter estimation and shot noise measurements.

We also evaluate the system performance at different underwater transmission distances with different water types, as shown in Fig. 6. The attenuation coefficients (c) of typical water types from [4,22] are also given in this figure, which is contributed from both the absorption and scattering of the light propagating through the water. It can be seen that the maximum secure key rate of the system can offer is about 1.15 Mbits/s for the back-to-back connection, and the secure key rates are reduced with increasing distance through the water channel. The performance of underwater CV-QKD system is degraded significantly as the water turbidity increases, since the transmitting weak quantum signal is sensitive to the loss of the water channel. At a transmission distance of 20 m, the secure key rate drops from about 303.04 kbits/s to 18.46 kbits/s when the turbidity of the water increased from c=0.043/m (pure sea water) to c=0.151/m (clear ocean water), and no secure key can be guaranteed with coastal ocean water and turbid harbor water. The maximum transmission distances of the secure keys significantly decrease with the increase of turbidity of the water, which are about 148.7 m, 42.3 m, 16.1 m, and 2.92 m in pure sea water, clear ocean water, coastal ocean water, and turbid harbor water respectively.

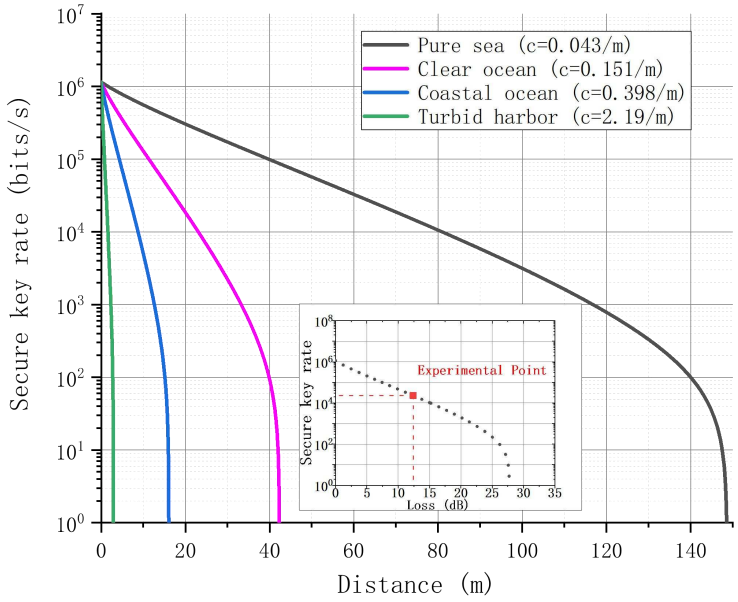

Fig. 6. The estimated secure key rate of the demonstrated underwater CV-QKD system as a function of distance with different water types. (The inset shows the estimated secure key rate as a function of channel loss and the red dot shows where the experimental point is.)

4. Conclusion

To the best of our knowledge, we have experimentally demonstrated the feasibility of an underwater CV-QKD system based on the four-state protocol for the first time. The parameter estimation is performed experimentally over a 6-meter water channel with a loss of 12.4 dB. The maximum shot noise to electronic noise ratio of about 13.14 dB can be obtained by the tested coherent receiver with 1.29$\times 10^7$ photons per pulse from LO. The estimated parameters T and ξ are

Optics EXPRESS

determined as about 0.0568 and 0.0088 SNU respectively on the block size of 4.57×10^6. The secure key rate is then estimated as 2.75×10^{-4} bits per pulse, which corresponds to the 22.9 kbits/s at the system repetition rate of 250 MHz. The underwater CV-QKD system performance in terms of the secure key rate at different transmission distance is also evaluated with typical water types. The demonstrated system has an achievable maximum transmission distance of 148.7 m in pure sea water.

Appendix. Symplectic Eigenvalues υ_i

The maximum information accessible to Eve in Eq.(2) is determined from the symplectic eigenvalues υ_i (i=1,2,3,4,5), which are given by [22,26]:

$$\upsilon_{1,2} = \sqrt{\frac{1}{2}\left(A \pm \sqrt{A^2 - 4B}\right)} \tag{A1}$$

$$\upsilon_{3,4} = \sqrt{\frac{1}{2}\left(C \pm \sqrt{C^2 - 4D}\right)} \tag{A2}$$

$$\upsilon_5 = 1 \tag{A3}$$

where A and B are expressed as:

$$A = V^2 + T^2(V + \chi_{\text{line}})^2 - 2TZ^2 \tag{A4}$$

$$B = (TV^2 + TV\chi_{\text{line}} - TZ^2)^2 \tag{A5}$$

with

$$Z = \mathrm{V}_A\left(\lambda_0^{\frac{3}{2}}\lambda_1^{-\frac{1}{2}} + \lambda_1^{\frac{3}{2}}\lambda_2^{-\frac{1}{2}} + \lambda_2^{\frac{3}{2}}\lambda_3^{-\frac{1}{2}} + \lambda_3^{\frac{3}{2}}\lambda_0^{-\frac{1}{2}}\right) \tag{A6}$$

where

$$\lambda_{0,2} = \frac{1}{2}e^{-\alpha^2}[\cosh(\alpha^2) \pm \cos(\alpha^2)] \tag{A7}$$

$$\lambda_{1,3} = \frac{1}{2}e^{-\alpha^2}[\sinh(\alpha^2) \pm \sin(\alpha^2)] \tag{A8}$$

For the case of homodyne detection, C and D are given by:

$$C = \frac{A\chi_{\text{hom}} + V\sqrt{B} + T(V + \chi_{\text{line}})}{T(V + \chi_{\text{tot}})} \tag{A9}$$

$$D = \sqrt{B}\frac{V + \sqrt{B}\chi_{\text{hom}}}{T(V + \chi_{\text{tot}})} \tag{A10}$$

Funding. The Major Key Project of PCL (PCL2022A02).

Acknowledgments. R. K. Acknowledges the support from EPSRC Quantum Communications Hub (Grant No. EP/T001011/1).

Disclosures. The authors declare that there are no conflicts of interest related to this article.

Data availability. Data underlying the results presented in this paper are not publicly available at this time but may be obtained from the authors upon reasonable request.

Optics EXPRESS

References

1. Z. Zeng, S. Fu, H. Zhang, Y. Dong, and J. Cheng, "A Survey of Underwater Optical Wireless Communications," IEEE Commun. Surv. Tutorials **19**(1), 204–238 (2017).
2. H. M. Oubei, C. Shen, A. Kammoun, E. Zedini, K.-H. Park, X. Sun, G. Liu, C. H. Kang, T. K. Ng, M.-S. Alouini, and B. S. Ooi, "Light based underwater wireless communications," Jpn. J. Appl. Phys. **57**(8S2), 08PA06 (2018).
3. F. Hanson and S. Radic, "High bandwidth underwater optical communication," Appl. Opt. **47**(2), 277–283 (2008).
4. M. Kong, J. Wang, Y. Chen, T. Ali, R. Sarwar, Y. Qiu, S. Wang, J. Han, and J. Xu, "Security weaknesses of underwater wireless optical communication," Opt. Express **25**(18), 21509–21518 (2017).
5. J. Wang, C. Lu, S. Li, and Z. Xu, "100 m/500 Mbps underwater optical wireless communication using an NRZ-OOK modulated 520 nm laser diode," Opt. Express **27**(9), 12171–12181 (2019).
6. C. Bennett and G. Brassard, "Quantum cryptography: Public key distribution and coin tossing," in *Proceedings of IEEE International Conference on Computers, Systems and Signal Processing* (1984), pp. 175–179.
7. M. Lucamarini, K. A. Patel, J. F. Dynes, B. Fröhlich, A. W. Sharpe, A. R. Dixon, Z. L. Yuan, R. V. Penty, and A. J. Shields, "Efficient decoy-state quantum key distribution with quantified security," Opt. Express **21**(21), 24550–24565 (2013).
8. D. Stucki, N. Brunner, N. Gisin, V. Scarani, and H. Zbinden, "Fast and simple one-way quantum key distribution," Appl. Phys. Lett. **87**(19), 194108 (2005).
9. F. Grosshans and P. Grangier, "Continuous Variable Quantum Cryptography Using Coherent States," Phys. Rev. Lett. **88**(5), 057902 (2002).
10. A. Leverrier and P. Grangier, "Unconditional Security Proof of Long-Distance Continuous-Variable Quantum Key Distribution with Discrete Modulation," Phys. Rev. Lett. **102**(18), 180504 (2009).
11. S.-K. Liao, W.-Q. Cai, W.-Y. Liu, L. Zhang, Y. Li, J.-G. Ren, J. Yin, Q. Shen, Y. Cao, Z.-P. Li, F.-Z. Li, X.-W. Chen, L.-H. Sun, J.-J. Jia, J.-C. Wu, X.-J. Jiang, J.-F. Wang, Y.-M. Huang, Q. Wang, Y.-L. Zhou, L. Deng, T. Xi, L. Ma, T. Hu, Q. Zhang, Y.-A. Chen, N.-L. Liu, X.-B. Wang, Z.-C. Zhu, C.-Y. Lu, R. Shu, C.-Z. Peng, J.-Y. Wang, and J.-W. Pan, "Satellite-to-ground quantum key distribution," Nature **549**(7670), 43–47 (2017).
12. N. Hosseinidehaj, Z. Babar, R. Malaney, S. X. Ng, and L. Hanzo, "Satellite-Based Continuous-Variable Quantum Communications: State-of-the-Art and a Predictive Outlook," IEEE Commun. Surv. Tutorials **21**(1), 881–919 (2019).
13. X. Tang, R. Kumar, S. Ren, A. Wonfor, R. V. Penty, and I. H. White, "Performance of continuous variable quantum key distribution system at different detector bandwidth," Opt. Commun. **471**, 126034 (2020).
14. Y. Wang, S. Zou, Y. Mao, and Y. Guo, "Improving Underwater Continuous-Variable Measurement-Device-Independent Quantum Key Distribution via Zero-Photon Catalysis," Entropy **22**(5), 571 (2020).
15. P. Shi, S.-C. Zhao, Y.-J. Gu, and W.-D. Li, "Channel analysis for single photon underwater free space quantum key distribution," J. Opt. Soc. Am. A **32**(3), 349–356 (2015).
16. S. Zhao, X. Han, Y. Xiao, Y. Shen, Y. Gu, and W. Li, "Performance of underwater quantum key distribution with polarization encoding," J. Opt. Soc. Am. A **36**(5), 883–892 (2019).
17. L. Ji, J. Gao, A.-L. Yang, Z. Feng, X.-F. Lin, Z.-G. Li, and X.-M. Jin, "Towards quantum communications in free-space seawater," Opt. Express **25**(17), 19795–19806 (2017).
18. Z. Feng, S. Li, and Z. Xu, "Experimental underwater quantum key distribution," Opt. Express **29**(6), 8725–8736 (2021).
19. S. Zhao, W. Li, Y. Shen, Y. Yu, X. Han, H. Zeng, M. Cai, T. Qian, S. Wang, Z. Wang, Y. Xiao, and Y. Gu, "Experimental investigation of quantum key distribution over a water channel," Appl. Opt. **58**(14), 3902–3907 (2019).
20. C.-Q. Hu, Z.-Q. Yan, J. Gao, Z.-M. Li, H. Zhou, J.-P. Dou, and X.-M. Jin, "Decoy-State Quantum Key Distribution Over a Long-Distance High-Loss Air-Water Channel," Phys. Rev. Appl. **15**(2), 024060 (2021).
21. D. D. Li, Q. Shen, W. Chen, Y. Li, X. Han, K. X. Yang, Y. Xu, J. Lin, C. Z. Wang, H. L. Yong, W. Y. Liu, Y. Cao, J. Yin, S. K. Liao, and J. G. Ren, "Proof-of-principle demonstration of quantum key distribution with seawater channel: towards space-to-underwater quantum communication," Opt. Commun. **452**, 220–226 (2019).
22. X. Ruan, H. Zhang, W. Zhao, X. Wang, X. Li, and Y. Guo, "Security Analysis of Discrete-Modulated Continuous-Variable Quantum Key Distribution over Seawater Channel," Appl. Sci. **9**(22), 4956 (2019).
23. Y. Guo, C. L. Xie, P. Huang, J. W. Li, L. Zhang, D. Huang, and G. H. Zeng, "Channel-parameter estimation for satellite-to-submarine continuous-variable quantum key distribution," Phys. Rev. A **97**(5), 052326 (2018).
24. C.-L. Xie, Y. Guo, Y.-J. Wang, D. Huang, and L. Zhang, "Security Simulation of Continuous-Variable Quantum Key Distribution over Air-to-Water Channel Using Monte Carlo Method," Chinese Phys. Lett. **35**(9), 090302 (2018).
25. Y. Mao, X. Wu, W. Huang, Q. Liao, H. Deng, Y. Wang, and Y. Guo, "Monte Carlo-Based Performance Analysis for Underwater Continuous-Variable Quantum Key Distribution," Appl. Sci. **10**(17), 5744 (2020).
26. H. Zhang, J. Fang, and G. He, "Improving the performance of the four-state continuous-variable quantum key distribution by using optical amplifiers," Phys. Rev. A **86**(2), 022338 (2012).
27. A. Becir, F. A. A. El-Orany, and M. R. B. Wahiddin, "Continuous-Variable Quantum Key Distribution Protocols With Eight-State Discrete Modulation," Int. J. Quantum Inf. **10**(01), 1250004 (2012).
28. A. S. Holevo, "Bounds for the quantity of information transmitted by a quantum communication channel," Problemy Peredachi Informatsii **9**(3), 3–11 (1973).
29. N. Saeed, A. Celik, T. Y. Al-Naffouri, and M.-S. Alouini, "Underwater optical wireless communications, networking, and localization: A survey," Ad Hoc Networks **94**, 101935 (2019).

Optics EXPRESS

30. X. Sun, M. Kong, O. Alkhazragi, C. Shen, E.-N. Ooi, X. Zhang, U. Buttner, T. K. Ng, and B. S. Ooi, "Non-line-of-sight methodology for high-speed wireless optical communication in highly turbid water," Opt. Commun. **461**, 125264 (2020).
31. A. Marie and R. Alléaume, "Self-coherent phase reference sharing for continuous-variable quantum key distribution," Phys. Rev. A **95**(1), 012316 (2017).
32. R. Kumar, H. Qin, and R. Alléaume, "Coexistence of continuous variable QKD with intense DWDM classical channels," New J. Phys. **17**(4), 043027 (2015).
33. X. Tang, R. Kumar, C. Sun, L. Zhang, Z. Chen, R. Jiang, H. Wang, and A. Zhang, "Towards underwater coherent optical wireless communications using a simplified detection scheme," Opt. Express **29**(13), 19340–19351 (2021).